Proceedings of the

9th International Conference on Climbing and Walking Robots

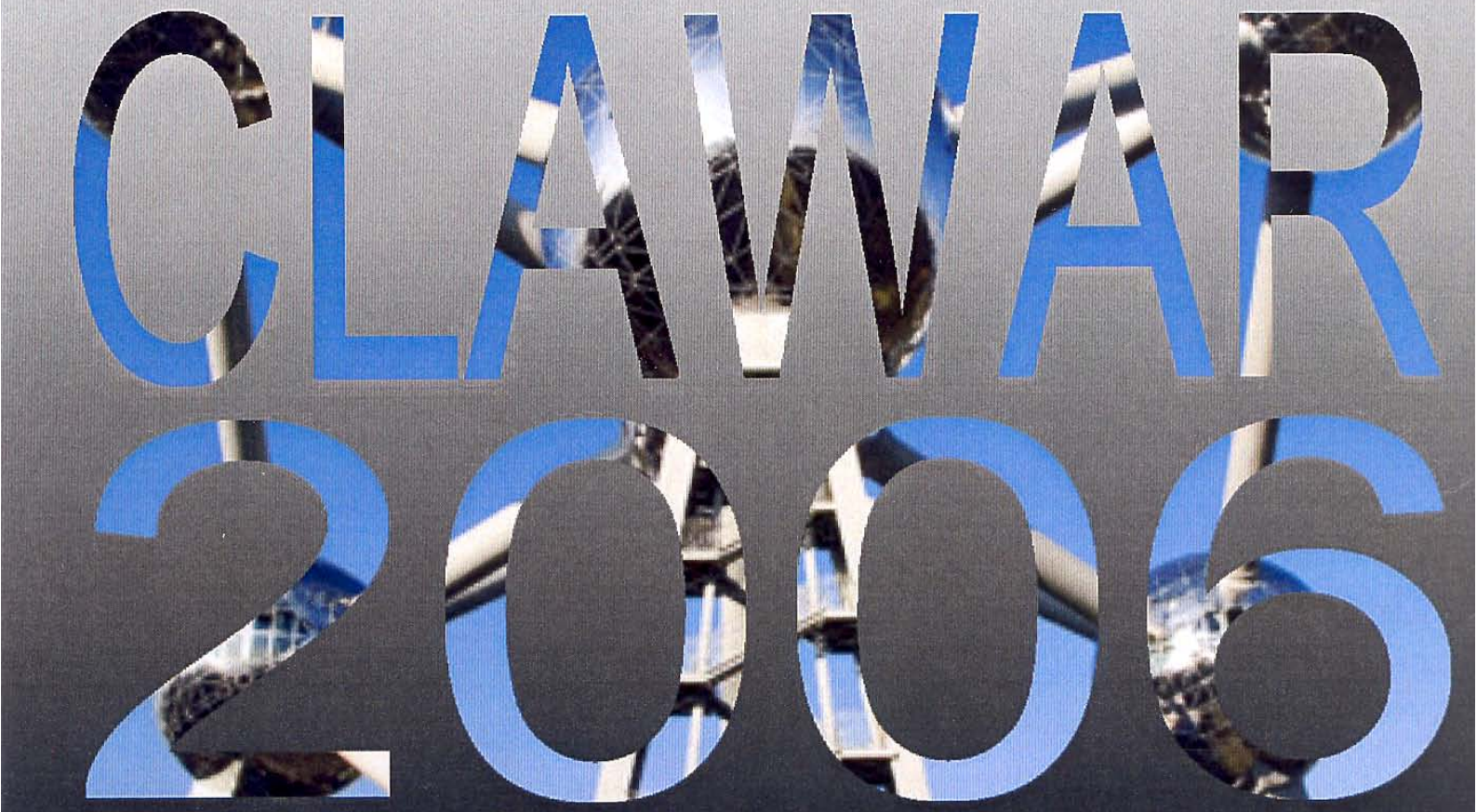

12-14 September 2006, Brussels, Belgium

Edited by Yvan Baudoin & Dirk Lefeber

Optimum Gait Selection for Quadruped Robots

Manuel F. Silva and J. A. Tenreiro Machado
Department of Electrical Engineering, Institute of Engineering of Porto,
Rua Dr. António Bernardino de Almeida – 4200-072 Porto – Portugal
email: mss@isep.ipp.pt, jtm@isep.ipp.pt

Abstract: **This paper studies periodic gaits of quadruped animals and its application to multilegged artificial locomotion systems. The purpose is to determine the best set of gait and locomotion variables during walking, for different robot velocities and intra-body compliance characteristics, based on two formulated performance measures. A set of experiments reveals the influence of the gait and locomotion variables upon the proposed indices, namely that the gait and the locomotion parameters should be adapted to the robot forward velocity and to the robot intra-body compliance characteristics.**

Keywords: **Robotics, locomotion, modelling, simulation**

I. INTRODUCTION

Walking machines allow locomotion in terrain inaccessible to other type of vehicles. In order for this to become possible, gait analysis and selection is a research area requiring an appreciable modelling effort for the improvement of mobility with legs in unstructured environments. Several robots have been developed which adopt different quadruped gaits such as the bound [1 – 3], trot [4] and gallop [5]. Nevertheless, detailed studies on the best set of gait and locomotion variables for different robot velocities are missing [6].

In this line of thought, a simulation model for multi-legged locomotion systems was developed, for several periodic gaits [7]. Based on this model, we test the quadruped robot locomotion, as a function of V_F, when adopting different periodic gaits often observed in several quadruped animals while they walk / run at variable speeds [8].

This study intends to generalize previous work [9, 10] through the formulation of two indices measuring the average energy consumption and the hip trajectory errors during forward straight line walking at different velocities. First, a set of simulation experiments are develop to estimate the optimum values for the parameters step length L_S and body height H_B, during the robot locomotion, while the robot is moving along the planned trajectories. Following the best locomotion gait in the velocity range $0.1 \le V_F \le 10.0$ ms^{-1} is determined, from the viewpoint of energy efficiency, being the controller tuned for each particular locomotion velocity, while minimizing the index E_{av}, and adopting the optimum locomotion parameters L_S and H_B determined previously. These experiments are repeated for distinct characteristics of the robot intra-body compliance.

Bearing these facts in mind, the paper is organized as follows. Section two introduces the robot kinematic model and the motion planning scheme. Sections three and four present the robot dynamic model and control architecture and the optimizing indices, respectively. Section five develops a set of experiments that reveal the influence of the locomotion parameters and robot gaits on the performance measures, as a function of robot body velocity. Finally, section six outlines the main conclusions.

II. KINEMATICS AND TRAJECTORY PLANNING

We consider a quadruped walking system (Figure 1) with $n = 4$ legs, equally distributed along both sides of the robot body, having each two rotational joints (*i.e.*, $j = \{1, 2\} \equiv \{\text{hip, knee}\}$).

Motion is described by means of a world coordinate system. The kinematic model comprises: the cycle time T, the duty factor β, the transference time $t_T = (1-\beta)T$, the support time $t_S = \beta T$, the step length L_S, the stroke pitch S_P, the body height H_B, the maximum foot clearance F_C, the i^{th} leg lengths L_{i1} and L_{i2} and the foot trajectory offset O_i ($i = 1, \ldots, n$). Moreover, we consider a periodic trajectory for each foot, with body velocity $V_F = L_S / T$.

Gaits describe sequences of leg movements, alternating between transfer and support phases. Given a particular gait and duty factor β, it is possible to calculate, for leg i, the corresponding phase ϕ_i, the time instant where each leg leaves and returns to contact with the ground and the cartesian trajectories of the tip of the feet (that must be completed during t_T) [7]. Based on this data, the trajectory generator is responsible for producing a motion that synchronizes and coordinates the legs.

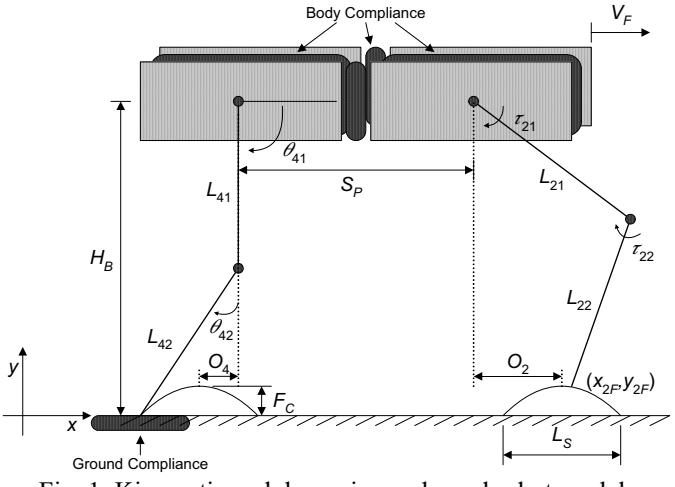

Fig. 1. Kinematic and dynamic quadruped robot model.

The robot body, and by consequence the legs hips, is assumed to have a desired horizontal movement with a constant forward speed V_F. Therefore, for leg i the cartesian coordinates of the hip of the legs are given by $\mathbf{p_{Hd}}(t) = [x_{iHd}(t), y_{iHd}(t)]^{\mathrm{T}}$:

$$\mathbf{p_{Hd}}(t) = \begin{bmatrix} V_F t + Sp\left(1 - \mathrm{ceil}(i/2)\right) & H_B \end{bmatrix}^{\mathrm{T}} \quad (1)$$

Regarding the feet trajectories, on a previous work we evaluated two alternative space-time foot trajectories, namely a cycloidal and a sinusoidal function [11]. It was demonstrated that the cycloid is superior to the sinusoidal function, since it improves the hip and foot trajectory tracking, while minimising the corresponding joint torques. However, a step acceleration profile is assumed for the feet trajectories. These results do not present significant changes for different acceleration profiles of the foot trajectory.

In order to avoid the impact and friction effects, at the planning phase we impose null velocities of the feet in the instants of landing and taking off, assuring also the velocity continuity.

Considering the above conclusions, for each cycle the desired geometric trajectory of the foot of the swing leg is computed through a cycloid function (Eq. 2). For example, considering that the transfer phase starts at $t = 0$ s for leg $i = 1$ we have for $\mathbf{p_{Fd}}(t) = [x_{iFd}(t), y_{iFd}(t)]^{\mathrm{T}}$:

- during the transfer phase:

$$\mathbf{p_{Fd}}(t) = \left[V_F \left[t - \frac{t_T}{2\pi} \sin\left(\frac{2\pi t}{t_T} \right) \right], \quad \frac{F_C}{2} \left[1 - \cos\left(\frac{2\pi t}{t_T} \right) \right] \right]^{\mathrm{T}} \quad (2)$$

- during the stance phase:

$$\mathbf{p_{Fd}}(t) = \begin{bmatrix} V_F T & 0 \end{bmatrix}^{\mathrm{T}} \quad (3)$$

The algorithm for the forward motion planning accepts the desired cartesian trajectories of the leg hips $\mathbf{p_{Hd}}(t)$ and feet $\mathbf{p_{Fd}}(t)$ as inputs and, by means of an inverse kinematics algorithm $\boldsymbol{\psi}^{-1}$, generates the related joint trajectories $\boldsymbol{\Theta_d}(t) = [\theta_{i1d}(t), \theta_{i2d}(t)]^{\mathrm{T}}$, selecting the solution corresponding to a forward knee:

$$\mathbf{p_d}(t) = \begin{bmatrix} x_{id}(t) & y_{id}(t) \end{bmatrix}^{\mathrm{T}} = \mathbf{p_{Fd}}(t) - \mathbf{p_{Hd}}(t) \quad (4a)$$

$$\mathbf{p_d}(t) = \boldsymbol{\psi}\left[\boldsymbol{\Theta_d}(t)\right] \Rightarrow \boldsymbol{\Theta_d}(t) = \boldsymbol{\psi}^{-1}\left[\mathbf{p_d}(t)\right] \quad (4b)$$

$$\dot{\boldsymbol{\Theta}}_{\mathbf{d}}(t) = \mathbf{J}^{-1}\left[\dot{\mathbf{p}}_{\mathbf{d}}(t)\right], \ \mathbf{J} = \frac{\partial \boldsymbol{\psi}}{\partial \boldsymbol{\Theta}_{\mathbf{d}}} \quad (4c)$$

III. Robot Dynamics and Control Architecture

A. Inverse Dynamics Computation

The planned joint trajectories constitute the reference for the robot control system. The model for the robot inverse dynamics is formulated as:

$$\boldsymbol{\Gamma} = \mathbf{H}(\boldsymbol{\Theta})\ddot{\boldsymbol{\Theta}} + \mathbf{c}\left(\boldsymbol{\Theta}, \dot{\boldsymbol{\Theta}}\right) + \mathbf{g}(\boldsymbol{\Theta}) - \mathbf{F_{RH}} - \mathbf{J_F^T}(\boldsymbol{\Theta})\mathbf{F_{RF}} \quad (5)$$

TABLE I

System Parameters

	Robot model parameters		Locomotion parameters
S_P	1 m	L_S	1 m
L_{ij}	0.5 m	H_B	0.9 m
O_i	0 m	F_C	0.1 m
M_b	88.0 kg		
M_{ij}	1 kg	**Ground parameters**	
K_{xH}	10^5 Nm^{-1}	K_{xF}	1.3×10^6 Nm^{-1}
K_{yH}	10^4 Nm^{-1}	K_{yF}	1.7×10^6 Nm^{-1}
B_{xH}	10^3 Nsm^{-1}	B_{xF}	2.3×10^6 Nsm^{-1}
B_{yH}	10^2 Nsm^{-1}	B_{yF}	2.7×10^6 Nsm^{-1}

where $\boldsymbol{\Gamma} = [f_{ix}, f_{iy}, \tau_{i1}, \tau_{i2}]^{\mathrm{T}}$ ($i = 1, \ldots, n$) is the vector of forces / torques, $\boldsymbol{\Theta} = [x_{iH}, y_{iH}, \theta_{i1}, \theta_{i2}]^{\mathrm{T}}$ is the vector of position coordinates, $\mathbf{H}(\boldsymbol{\Theta})$ is the inertia matrix and $\mathbf{c}\left(\boldsymbol{\Theta}, \dot{\boldsymbol{\Theta}}\right)$ and $\mathbf{g}(\boldsymbol{\Theta})$ are the vectors of centrifugal / Coriolis and gravitational forces / torques, respectively. The $n \times m$ ($m = 2$) matrix $\mathbf{J_F^T}(\boldsymbol{\Theta})$ is the transpose of the robot Jacobian matrix, $\mathbf{F_{RH}}$ is the $m \times 1$ vector of the body inter-segment forces and $\mathbf{F_{RF}}$ is the $m \times 1$ vector of the reaction forces that the ground exerts on the robot feet. These forces are null during the foot transfer phase. During the system simulation, Eq. (5) is integrated through the Runge-Kutta method.

We consider that the joint actuators are not ideal, exhibiting a saturation given by:

$$\tau_{ijm} = \begin{cases} \tau_{ijC} & , \ |\tau_{ijm}| \le \tau_{ijMax} \\ \mathrm{sgn}\left(\tau_{ijC}\right) \cdot \tau_{ijMax} & , \ |\tau_{ijm}| > \tau_{ijMax} \end{cases} \quad (6)$$

where, for leg i and joint j, τ_{ijC} is the controller demanded torque, τ_{ijMax} is the maximum torque that the actuator can supply and τ_{ijm} is the motor effective torque.

B. Robot Body Model

Figure 1 presents the dynamic model for the hexapod body and foot-ground interaction. It is considered robot body compliance because most walking animals have a spine that allows supporting the locomotion with improved stability. In the present study, the robot body is divided in n identical segments (each with mass $M_b n^{-1}$) and a linear spring-damper system is adopted to implement the intra-body compliance according to:

$$f_{i\eta H} = \sum_{i'=1}^{u} \left[-K_{\eta H}\left(\eta_{iH} - \eta_{i'H}\right) - B_{\eta H}\left(\dot{\eta}_{iH} - \dot{\eta}_{i'H}\right) \right] \quad (7)$$

where $(x_{i'H}, y_{i'H})$ are the hip coordinates and u is the total number of segments adjacent to leg i.

In this study, the parameters $K_{\eta H}$ and $B_{\eta H}$ ($\eta = \{x, y\}$) in the {horizontal, vertical} directions, respectively, are defined so that the body behaviour is similar to the one expected to occur on an animal (Table I).

C. Foot-Ground Interaction Model

The contact of the i^{th} robot feet with the ground is modelled through a non-linear system [11] with linear stiffness $K_{\eta F}$ and non-linear damping $B_{\eta F}$ ($\eta = \{x, y\}$) in the {horizontal, vertical} directions, respectively (see Figure 1), yielding:

$$f_{i\eta F} = -K_{\eta F}\left(\eta_{iF} - \eta_{iF0}\right) - B_{\eta F}\left[-\left(y_{iF} - y_{iF0}\right)\right]^{v_\eta}\left(\dot{\eta}_{iF} - \dot{\eta}_{iF0}\right)$$
$$v_x = 1.0,\ v_y = 0.9 \tag{8}$$

where x_{iF0} and y_{iF0} are the coordinates of foot i touchdown and v_η ($\eta = \{x, y\}$) is a parameter dependent on the ground characteristics. The values for the parameters $K_{\eta F}$ and $B_{\eta F}$ (Table I) are based on the studies of soil mechanics [11].

D. Control Architecture

The general control architecture of the hexapod robot is presented in Figure 2. In the control architecture implemented for this simulation model, the trajectory planning is carried out in the cartesian space but the control is performed in the joint space, which requires the integration of the inverse kinematic model in the forward path. The control algorithm includes an external position feedback loop and an internal loop with information of the foot-ground interaction force.

On a previous work were demonstrated the advantages of this cascade controller, with PD position control and foot force feedback, over a classical PD with, merely, position feedback, particularly in real situations where we have non-ideal actuators with saturation and being also more robust for variable ground characteristics [4].

For $G_{c1}(s)$ we adopt a PD controller and for G_{c2} a simple P controller. For the PD algorithm we have:

$$G_{C1\,j}(s) = Kp_j + Kd_j s, \quad j = 1,2 \tag{9}$$

being Kp_j and Kd_j the proportional and derivative gains.

IV. Measures for Performance Evaluation

In mathematical terms we establish two global measures of the overall performance of the mechanism in an average sense. In this perspective, we define one index $\{E_{av}\}$ inspired on the system dynamics and another one $\{\varepsilon_{xyH}\}$ based on the trajectory tracking errors.

Regarding the mean absolute density of energy per travelled distance E_{av}, it is computed assuming that energy regeneration is not available by actuators doing negative work (by taking the absolute value of the power). At a given joint j (each leg has $m = 2$ joints) and leg i (since we are adopting a quadruped it yields $n = 4$ legs), the mechanical power is the product of the motor torque and angular velocity. The global index E_{av} is obtained by averaging the mechanical absolute energy delivered over the travelled distance d:

$$E_{av} = \frac{1}{d}\sum_{i=1}^{n}\sum_{j=1}^{m}\int_0^T \left|\boldsymbol{\tau}_{ij}(t)\,\dot{\boldsymbol{\theta}}_{ij}(t)\right| dt \quad \left[\mathrm{Jm}^{-1}\right] \tag{10}$$

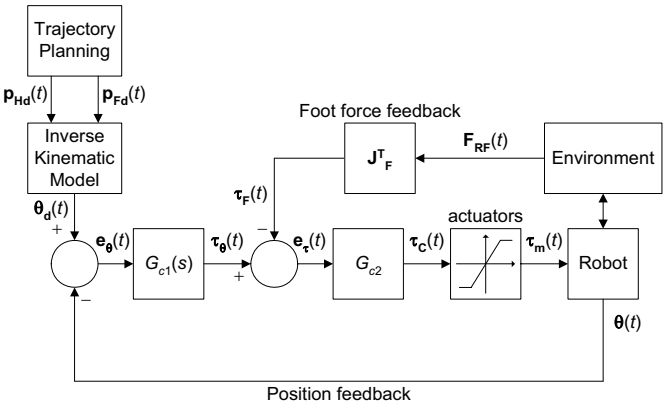

Fig. 2. Quadruped robot control architecture.

TABLE II

Quadruped Controller Parameters

Gait	ϕ_1	ϕ_2	ϕ_3	ϕ_4	β
Walk	0	0.5	0.75	0.25	0.65
Chelonian Walk	0	0.5	0.5	0	0.8
Amble	0	0.5	0.75	0.25	0.45
Trot	0	0.5	0.5	0	0.4
Pace	0	0.5	0	0.5	0.4
Canter	0	0.3	0.7	0	0.4
Transverse Gallop	0	0.2	0.6	0.8	0.3
Rotary Gallop	0	0.1	0.6	0.5	0.3
Half-Bound	0.7	0.6	0	0	0.2
Bound	0	0	0.5	0.5	0.2

In what concerns the hip trajectory following errors we define the index:

$$\varepsilon_{xyH} = \sum_{i=1}^{n}\sqrt{\frac{1}{N_s}\sum_{k=1}^{N_s}\left(\Delta_{ixH}{}^2 + \Delta_{iyH}{}^2\right)} \quad [\mathrm{m}]$$
$$\Delta_{ixH} = x_{iHd}(k) - x_{iH}(k),\ \Delta_{iyH} = y_{iHd}(k) - y_{iH}(k) \tag{11}$$

where N_s is the total number of samples for averaging purposes and $\{d, r\}$ indicate the i^{th} samples of the desired and real position, respectively.

In all cases the performance optimization requires the minimization of each index.

V. Simulation Results

To illustrate the use of the preceding concepts, in this section we develop a set of simulation experiments to estimate the influence of parameters L_S and H_B, when adopting periodic gaits [8]. We consider three walking gaits (Walk, Chelonian Walk and Amble), two symmetrical running gaits (Trot and Pace) and five asymmetrical running gaits (Canter, Transverse Gallop, Rotary Gallop, Half-Bound and Bound). These gaits are usually adopted by animals moving at low, moderate and high speed, respectively, being their main characteristics presented in Table II.

In a first phase, we develop a set of simulation experiments to estimate the optimum values for the parameters step length L_S and body height H_B with V_F, during the robot locomotion,

when adopting the periodic gaits and while the robot is moving along the planned trajectories.

In a second phase we determine the best locomotion gait, from the viewpoint of energy efficiency, in the velocity range $0.1 \leq V_F \leq 10.0$ ms^{-1}. The controller is tuned for each particular locomotion velocity, while minimizing the index E_{av}, first keeping the locomotion parameters L_S = 1.0 m and H_B = 0.9 m fixed and, on a second phase, adopting the optimum locomotion parameters L_S and H_B determined previously. These experiments are repeated for distinct values of the robot intra-body compliance parameters, since animals use their body compliance to store energy at high velocities

For the system simulation we consider the robot body parameters, the locomotion parameters and the ground parameters presented in Table I. Moreover, we assume high performance joint actuators with a maximum torque of τ_{ijMax} = 400 Nm. To tune the controller we adopt a systematic method, testing and evaluating a grid of several possible combinations of controller parameters, while minimising E_{av} (Eq. (10)).

A. Locomotion Parameters versus Body Forward Velocity

In order to analyse the evolution of the locomotion parameters L_S and H_B with V_F, we test the forward straight line quadruped planned robot locomotion, as a function of V_F, when adopting different gaits often observed in several quadruped animals while they walk / run at variable speeds [8].

With this purpose, the robot forward straight line planned locomotion is simulated for different gaits, while varying the body velocity on the range $0.2 \leq V_F \leq 10.0$ ms^{-1}. For each gait and body velocity, the set of locomotion parameters (L_S, H_B) that minimises the performance index E_{av} is determined.

The chart presented in Figure 3 depicts the minimum value of the index E_{av}, on the range of V_F under consideration, for three different robot gaits. It is possible to conclude that the minimum values of the index E_{av} increase with V_F, independently of the adopted locomotion gait. It is also possible to conclude that gaits with higher values of the duty factor β show a higher increase for the values of the performance index E_{av}. Although not presented here, due to space limitations, the behaviour of the charts min[$E_{av}(V_F)$], for all other gaits present similar shapes.

Next we analyse how the locomotion parameters vary with V_F. Figure 4 shows, for three locomotion gaits, that the optimal value of L_S must increase with V_F when considering the performance index E_{av}. The next figure (Figure 5) shows that H_B must decrease with V_F from the viewpoint of the same performance index.

For the other periodic walking gaits considered on this study, the evolution of the optimization index E_{av} and the locomotion parameters (L_S, H_B) with V_F follows the same pattern. Therefore, we conclude that the locomotion parameters should be adapted to the walking velocity in order to optimize the robot performance. As V_F increases, the value of H_B should be decreased and the value of L_S increased. These results seem to agree with the observations of the living quadruped creatures [12].

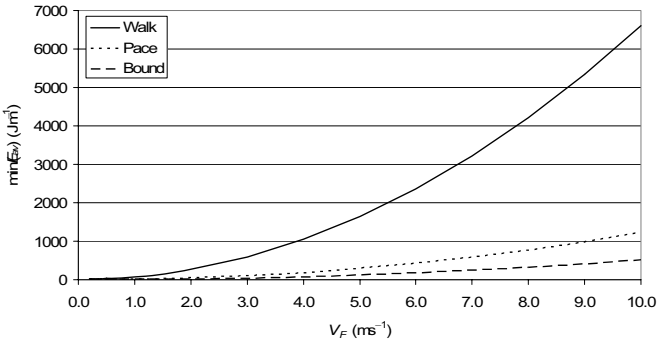

Fig. 3. min[$E_{av}(V_F)$] for F_C = 0.1 m.

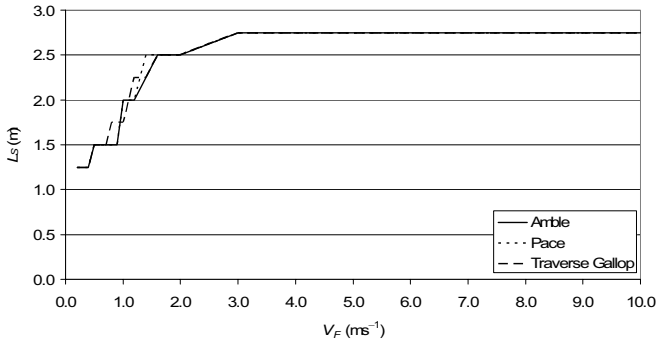

Fig. 4. $L_S(V_F)$ for min(E_{av}), with F_C = 0.1 m.

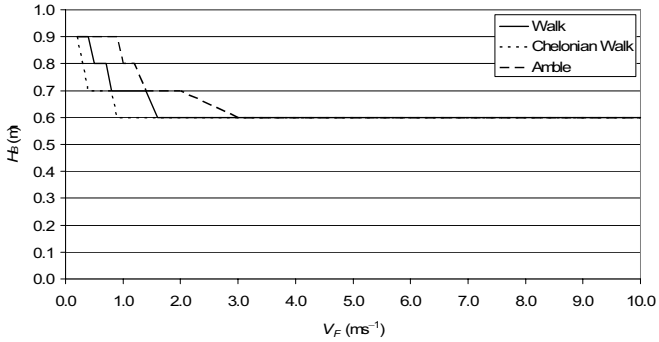

Fig. 5. $H_B(V_F)$ for min(E_{av}), with F_C = 0.1 m.

B. Gait Selection versus Body Forward Velocity Keeping L_S and H_B Fixed

In a second phase we determine the best locomotion gait, from the viewpoint of energy efficiency, at each forward robot velocity on the range $0.1 \leq V_F \leq 10.0$ ms^{-1}. For this phase of the study, the controller is tuned for each particular locomotion velocity, while minimizing the index E_{av}, and adopting the locomotion parameters L_S = 1.0 m and H_B = 0.9 m.

Figure 6 presents the charts of min[$E_{av}(V_F)$] and Figure 7 the minimum values of ε_{xyH} for the different gaits. The index E_{av} suggests that the locomotion should be Amble, Bound and Half-Bound as the speed increases. The other gaits under consideration present values of min[$E_{av}(V_F)$] higher than these ones, on all range of V_F under consideration. In particular, the gaits Walk and Chelonian Walk present the higher values of this performance measure.

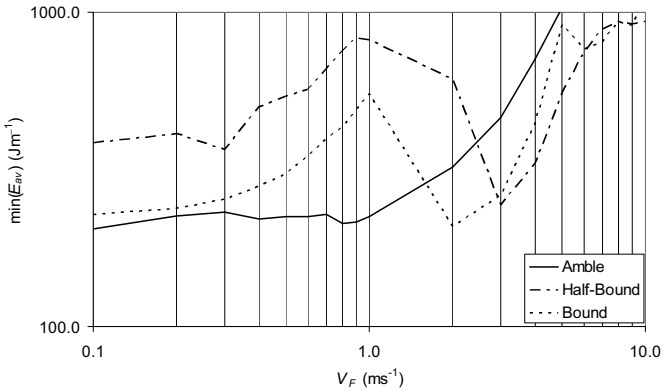

Fig. 6. min[$E_{av}(V_F)$] for F_C = 0.1 m, with L_S = 1.0 m and H_B = 0.9 m.

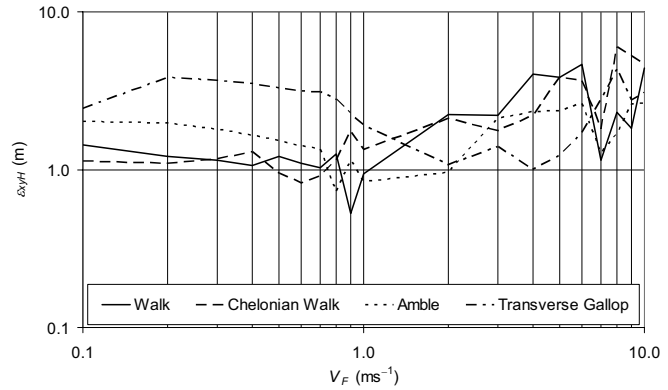

Fig. 7. min[$\varepsilon_{xyH}(V_F)$], for F_C = 0.1 m, with L_S = 1.0 m and H_B = 0.9 m.

Analysing the locomotion though the index ε_{xyH}, we verify that for low values of V_F (V_F < 1 ms^{-1}), the gaits Walk and Chelonian Walk allow the lower oscillations of the hips. For increasing values of the locomotion velocity the Amble and Transverse Gallop gaits present the lower values of ε_{xyH}.

C. Gait Selection versus Body Forward Velocity Varying L_S and H_B

In order to analyse the influence of the optimization of the locomotion parameters L_S and H_B on the locomotion performance, in the sequel we determine the best locomotion gait, from the viewpoint of the minimization of the index E_{av}, at each forward robot velocity on the range $0.1 \le V_F \le 10.0$ ms^{-1}. To conduct this study, the controller is tuned for each particular locomotion velocity, while minimizing the index E_{av}, and adopting for each gait at each tested value of V_F the locomotion parameters L_S and H_B determined at section V.*A*.

Figure 8 presents the chart of min[$E_{av}(V_F)$]. This index points out that the locomotion should be Amble, Trot and Bound as the speed increases. The other gaits under consideration present values of min[$E_{av}(V_F)$] higher than these ones, on all range of V_F under consideration. In particular, and once again, the gaits Walk and Chelonian Walk present the higher values of this performance measure.

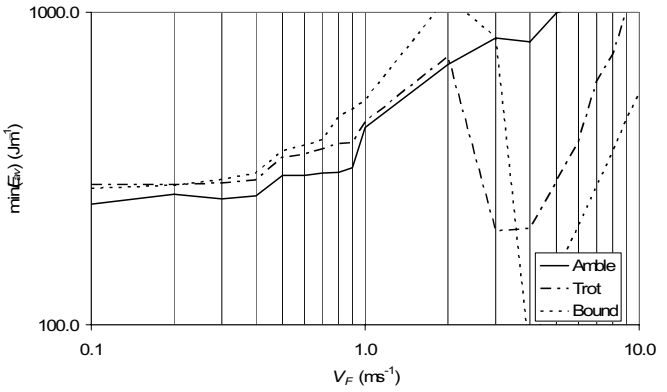

Fig. 8. min[$E_{av}(V_F)$] for F_C = 0.1 m, considering the optimum values of L_S and H_B.

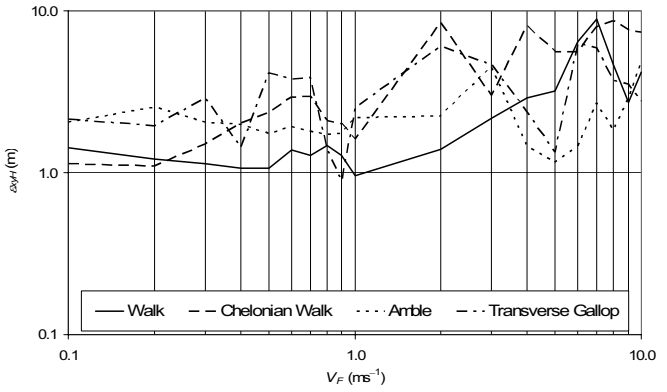

Fig. 9. min[$\varepsilon_{xyH}(V_F)$], for F_C = 0.1 m, considering the optimum values of L_S and H_B.

Comparing the results for this case with those for the previous one, we may conclude that for the Trot and Bound gaits there is a decrease in the values of E_{av} for V_F > 2 ms^{-1}. Therefore, by correctly choosing the gait to adopt and optimising correspondingly the locomotion parameters L_S and H_B the quadruped robot can move with increased performance.

From the viewpoint of the performance index ε_{xyH} (Figure 9), we verify that for low values of V_F (V_F < 0.2 ms^{-1}), the gait Chelonian Walk allows the lower oscillations of the hips. For medium values of V_F (0.2 ms^{-1} < V_F < 2 ms^{-1}), it is the Walk gait that presents the lower values of ε_{xyH}. For high values of the locomotion velocity (V_F > 3.0 ms^{-1}), the Amble and Transverse Gallop gaits allow the lower oscillations of the hips.

D. Gait Selection versus Body Forward Velocity for Stiff Body

The experiments performed in the previous section are now repeated for the case of assuming a stiff robot body. For this case, and considering the base parameters presented in Table I, the values of the intra-compliance defining parameters {K_{xH}, B_{xH}, K_{yH} and B_{yH}} are varied simultaneously through a multiplying factor K_{mult} = 10. For this case, the charts of min[$E_{av}(V_F)$] and of min[$\varepsilon_{xyH}(V_F)$], for the different gaits, are presented in Figures 10 and 11, respectively.

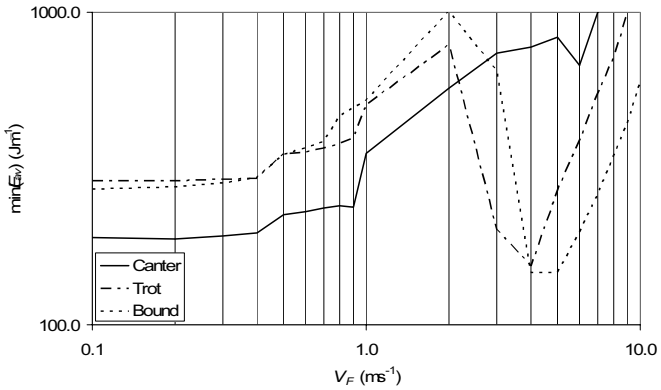

Fig. 10. min[$E_{av}(V_F)$] for F_C = 0.1 m, considering the optimum values of L_S and H_B.

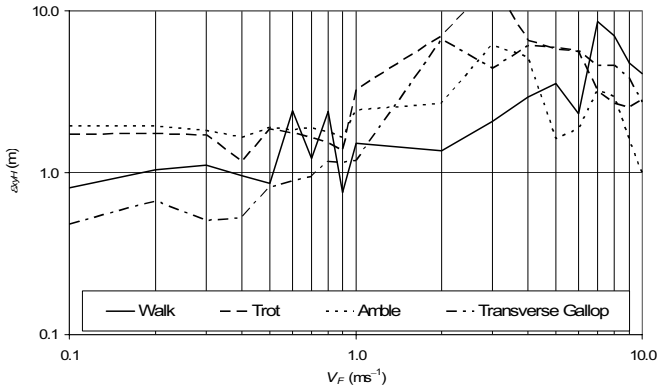

Fig. 11. min[$\varepsilon_{xyH}(V_F)$], for F_C = 0.1 m, considering the optimum values of L_S and H_B.

From the analysis of Figure 10, it is concluded that the most efficient way to perform the locomotion, measured through the index E_{av}, is to adopt the canter gait for $V_F < 2.0$ ms^{-1}), the Trot gait for 2.0 ms^{-1} < V_F < 4.0 ms^{-1} and the Bound gait for V_F > 4.0 ms^{-1}. All the remaining gaits under study present values of min[$E_{av}(V_F)$] higher than these ones, on all range of V_F under consideration.

Such as in the previous case, we observe that for values of V_F > 2 ms^{-1} there is a pronounced decrease in the values of min[$E_{av}(V_F)$] for the Trot and Bound gaits.

Concerning the locomotion performance, analysed from the viewpoint of the performance index ε_{xyH} (Figure 11), we conclude that for increasing values of the locomotion velocity the gaits Transverse Gallop (for V_F < 0.8 ms^{-1}), Walk (for 0.9 ms^{-1} < V_F < 4.0 ms^{-1}) and Amble (for V_F > 5.0 ms^{-1}) are the ones that allow the lower oscillations of the hips.

E. Gait Selection versus Body Forward Velocity for Soft Body

Finally, the study that is being developed is repeated for the case of assuming a soft robot body. For this case, and considering the base parameters presented in Table I, the values of the intra-compliance defining parameters {K_{xH}, B_{xH}, K_{yH} and B_{yH}} are varied simultaneously through a multiplying factor K_{mult} = 0.1.

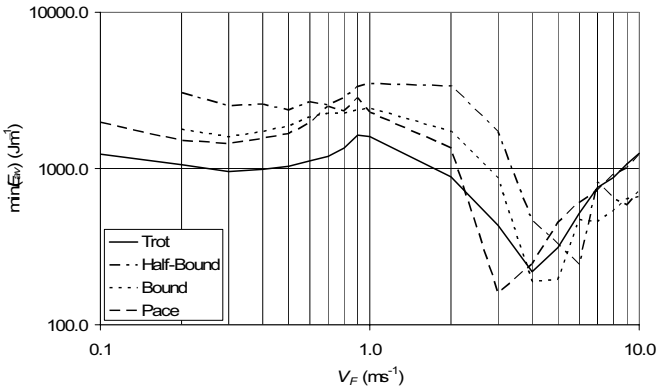

Fig. 12. min[$E_{av}(V_F)$] for F_C = 0.1 m, considering the optimum values of L_S and H_B.

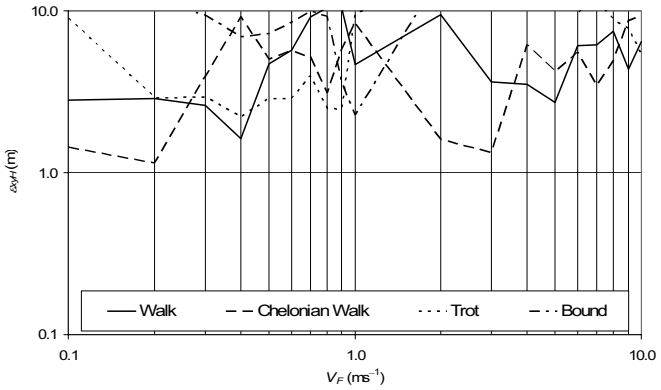

Fig. 13. min[$\varepsilon_{xyH}(V_F)$], for F_C = 0.1 m, considering the optimum values of L_S and H_B.

Figure 12 presents the charts of min[$E_{av}(V_F)$] and Figure 13 the charts of min[$\varepsilon_{xyH}(V_F)$] for the different gaits. The index E_{av} suggests that the locomotion should be Trot, Pace, Bound and Half-Bound as the speed increases. The other gaits under consideration present values of min[$E_{av}(V_F)$] higher than these ones, on all range of V_F under consideration.

Analysing the locomotion though the index ε_{xyH} we verify that, on most of the range of V_F under consideration, the gaits Walk and Chelonian Walk allow the lower oscillations of the hips. For medium values of the locomotion velocity (for 0.5 ms^{-1} < V_F < 2.0 ms^{-1}) the Trot and Bound gaits present the lower values of ε_{xyH}.

Comparing the results for this situation, with the ones for the previous cases, it is observed that for values of V_F < 2.0 ms^{-1} a soft body demands higher values of min[$E_{av}(V_F)$] for implementing the locomotion and the hip trajectory following errors, measured through ε_{xyH}, are also higher on all V_F range under study.

F. Discussion of the Results

From these above presented results, we can conclude that, from the viewpoint of each proposed optimising index, the robot gait should change with the desired forward body velocity. These results seem to agree with the observations of the living quadruped creatures [12].

In general terms, the values of min[$E_{av}(V_F)$] for the robot locomotion increase with V_F. This increase is more

pronounced for the walking gaits (Walk, Chelonian Walk and Amble). For the case of the running gaits (Trot, Pace, Canter, Transverse Gallop, Rotary Gallop, Half-Bound and Bound) there is a minimum of this index for values of $V_F > 0.9$ ms^{-1}, being this minimum more pronounced in case the locomotion parameters L_S and H_B are adapted to the locomotion velocity.

Concerning the minimum values of the performance index ε_{xyH}, we conclude that the walking gaits (Walk, Chelonian Walk and Amble) allow the locomotion with lower hip trajectories oscillations, and the asymmetrical running gaits (in particular the Half-Bound and Bound) impose the higher oscillations in the hips trajectories.

In conclusion, the locomotion gait and the parameters L_S and H_B should be chosen according to the intended robot forward velocity (generally, the value of L_S should be increased and the value of H_B decreased) in order to optimize the energy efficiency or the oscillation of the hips trajectories.

VI. Conclusions

In this paper we have compared several aspects of periodic quadruped locomotion gaits. By implementing different motion patterns, we estimated how the robot responds to the locomotion parameters step length and body height and to the forward speed.

For analyzing the system performance two quantitative measures were defined based on the system energy consumption and on the hip trajectory errors.

A set of experiments determined the best set of gait and locomotion variables, as a function of the forward velocity V_F, and for different characteristics of the robot body intra-compliance.

The results show that the locomotion parameters should be adapted to the walking velocity in order to optimize the robot performance. As the forward velocity increases, the value of L_S should be increased and the value of H_B decreased. Furthermore, for the case of a quadruped robot, we concluded that the gait should be adapted to V_F.

While our focus has been on a dynamic analysis in periodic gaits, certain aspects of locomotion are not necessarily captured by the proposed measures. Consequently, future work in this area will address the refinement of our models to incorporate more unstructured terrains, namely with distinct characteristics of the ground. Moreover, we plan to develop this analysis process in just one phase, simultaneously finding the optimum values of the locomotion parameters L_S and H_B and of the gait, versus V_F, through the use of a genetic algorithm.

Acknowledgements

The first author would like to acknowledge the Financial Support of Fundação Calouste Gulbenkian for his participation in the CLAWAR 2006 Conference.

References

[1] I. Poulakakis, J. A. Smith and M.Buehler, *Experimentally Validated Bounding Models for the Scout II Quadruped Robot*, Proceedings of the 2004 IEEE International Conference on Robotics & Automation (ICRA'2004), New Orleans, USA, 26 April – 1 May, 2004.

[2] Z. G. Zhang, Y. Fukuoka and H. Kimura, *Stable Quadrupedal Running Based on a Spring-Loaded Two-Segmented Legged Model*, Proceedings of the 2004 IEEE International Conference on Robotics & Automation (ICRA'2004), New Orleans, USA, 26 April – 1 May, 2004.

[3] F. Iida and R. Pfeifer, *"Cheap" Rapid Locomotion of a Quadruped Robot: Self-Stabilization of Bounding Gait*, Proceedings of the 8th Conference on Intelligent Autonomous Systems (IAS'2004), Amsterdam, The Netherlands, 10-13 March, 2004.

[4] N. Kohl and P. Stone, *Policy Gradient Reinforcement Learning for Fast Quadrupedal Locomotion*, Proceedings of the 2004 IEEE International Conference on Robotics & Automation (ICRA'2004), New Orleans, USA, 26 April – 1 May, 2004.

[5] L. R. Palmer, D. E. Orin, D. W. Marhefka, J. P. Schmiedeler and K. J. Waldron, *Intelligent Control of an Experimental Articulated Leg for a Galloping Machine*, Proceedings of the 2003 IEEE International Conference on Robotics & Automation (ICRA'2003), Taipei, Taiwan, 14-19 September, 2003.

[6] M. Hardt and O. von Stryk, *Towards Optimal Hybrid Control Solutions for Gait Patterns of a Quadruped*, Proceedings 3rd International Conference on Climbing and Walking Robots (CLAWAR 2000), Madrid, Spain, 2 – 4 October, 2000.

[7] M. F. Silva, J. A. T. Machado and A. M. Lopes, *Modelling and Simulation of Artificial Locomotion Systems*, ROBOTICA, **23**, pp. 595 – 606, 2005.

[8] URL: http://www.biology.leeds.ac.uk/teaching/3rdyear/Blgy3120/Jmvr/ /Loco/Gaits/GAITS.htm **[2006-08-09]**

[9] M. F. Silva, J. A. T. Machado, A. M. Lopes and J. K. Tar, *Gait Selection for Quadruped and Hexapod Walking Systems*, Proceedings of the 2004 IEEE International Conference on Computational Cybernetics (ICCC'2004), Vienna, Austria, 30 August – 1 September, 2004.

[10] M. F. Silva, J. A. T. Machado and A. M. Lopes, *Energy Efficiency of Quadruped Gaits*, Climbing and Walking Robots, M. O. Tokhi, G. S. Virk and M. A. Hossain (Eds.), Springer, pp. 735–742, 2006.

[11] M. F. Silva, J. A. T. Machado and A. M. Lopes, *Position / Force Control of a Walking Robot*, Machine Intelligence and Robotic Control, vol. 5, no. 2, pp. 33–44, 2003.

[12] R. McN. Alexander, *The Gaits of Bipedal and Quadrupedal Animal*, The International Journal of Robotics Research, vol. 3, no. 2, pp. 49–59, 1984.